Theory of Spatial Patterns of Intracellular Organelles

Anh-Tuan Dinh, Chinmay Pangarkar, Theo Theofanous, and Samir Mitragotri
Department of Chemical Engineering, University of California, Santa Barbara, California 93106

ABSTRACT Here we report on a generalized theory of spatial patterns of intracellular organelles, which are controlled by cells using cytoskeleton-based movements powered by molecular motors. The theory reveals that organelles exhibit one of the four distinct, stable patterns, namely aggregation, hyperdispersion, radial dispersion, and areal dispersion. Existence of specific patterns is determined by the contributions from three transport mechanisms, characterized by two Peclet numbers. The predicted patterns compare well with experimental data. This study provides a firm theoretical ground for classification of spatial patterns of organelles and understanding their regulation by cells.

Received for publication 6 February 2006 and in final form 28 February 2006.

Address reprint requests and inquiries to Prof. Samir Mitragotri, Dept. of Chemical Engineering, University of California, Santa Barbara, CA 93106. Tel.: 805-893-7532; Fax: 805-893-4731; E-mail: samir@engineering.ucsb.edu.

Spatial organization and compartmentalization of intracellular organelles such as endocytic vesicles (endosomes, lysosomes), mRNA granules, and mitochondria are central to many cellular functions, including trafficking of nutrients. To regulate spatial distribution of intracellular vesicles, cells utilize motor-assisted transport on cytoskeletal filaments, namely microtubules and actin filaments (1,2). At the operational level, the spatial distribution of organelles is controlled by activities of three motor proteins—kinesins, dyneins, and myosins—which are globally regulated by elaborate biochemical networks. In other words, a specific organization of organelles is a ''signature'' of complex interactions among many motors, organelles, and cytoskeletal filaments. Numerous studies have been performed to explore the biochemical and physical aspects of organelle transport; however, a global, quantitative relationship between spatial patterns of organelles (the effect) and motor activities (the cause) is not to be found in the literature. In this Letter, we report a generalized theory that establishes the cause-effect relationships of spatial organelle patterns. We show that all organelle patterns in nature can be characterized by two dimensionless parameters, the one- and two-dimensional Peclet numbers. A regime map of distinct organelle patterns is then constructed and compared to a broad range of experimental observations.

The focus is placed on organelle transport in nonpolarized cells. The system under consideration is illustrated in Fig. 1. Since cell thickness under culture conditions is often much smaller than other dimensions, cells can be approximated as two-dimensional circular disks. Organelles are allowed to move between the cell boundary (R_C) and the nuclear boundary (R_N). Viewing from the top, microtubules (MTs) grow radially from the microtubule-organizing center located at the cell center, creating a uniform two-dimensionsal array (1). Retrograde and ante-retrograde movements on MTs are mediated by dyneins and kinesins, which transport organelles toward and away from the cell center, respectively. Actin filaments (AFs) are shorter, and their distribution and orientation are random throughout the cytoplasm (3). Myosin-driven transport on randomized networks of AFs is often regarded as a form of facilitated diffusion (4).

To devise the equations for nonequilibrium motor-driven transport, we approximate the movements of organelles as stochastic trajectories of independent discrete particles, which continuously undergo first-order transitions from one transport state to another (5–7). For most intracellular organelles, this approximation is reasonable. The simplest state map that captures the key features of organelle transport reported in literature is depicted in Fig. 1 *b*. An organelle can switch intermittently between four distinct transport states, namely $s = 0$, free diffusion in cytosol; $s = +1$, kinesin-driven transport toward MT plus-ends; $s = -1$, dynein-driven transport toward MT minus-ends; and $s = 2$, myosin-driven transport on AFs. The state diagram implies that an organelle must detach from a filament before binding to another filament of the same or different type. Although direct switching between filaments is theoretically possible, no firm experimental evidence exists to support this behavior as a general rule. The assumption made here represents a reasonable approximation that is consistent with experimental data. The activities of molecular motors are represented by the rates of organelle binding to and detachment from the filaments, k_s and k'_s, respectively. These rates are lumped representations of complex interactions among motors, filaments and organelles. k_s and k'_s can be directly estimated from the run lengths and the motility fractions, often reported in particle-tracking experiments. The affinity constant, $K_s = k_s/k'_s$, reflects the likelihood that an organelle associates with a certain transport state.

Based on the depicted transition map and following the modeling approach reported in (1,7–9), we obtain a system

doi: 10.1529/biophysj.106.082875

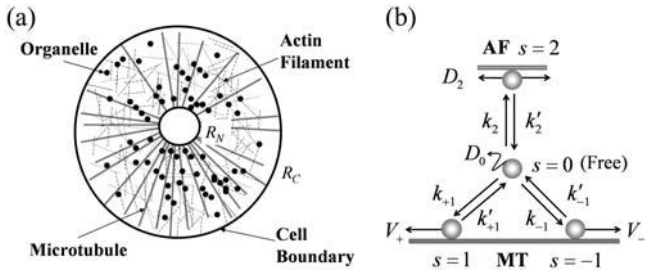

FIGURE 1 (*a*) Two-dimensional representation of cells. R_C and R_N represent the cell and nuclear boundaries, respectively. (*b*) Transition between motion states ($s = 0$, free diffusion in cytosol; $s = +1$, kinesin-driven transport toward MT plus-ends; $s = -1$, dynein-driven transport toward MT minus-ends; and $s = 2$, myosin-driven transport on AFs). V_+ and V_- are the velocities of MT-dependent movements. k_s and k_s' are the rates of organelles binding to and detachment from filaments. D_0 and D_2 are coefficients of free diffusion in cytoplasm and AF-dependent quasidiffusion.

of macroscopic mass conservation equations for organelle density $\tilde{c}_s(r,t)$ (No. of organelles at state s per unit area of cell, at radial position r and time t) as follows:

$$\partial_t\tilde{\boldsymbol{c}}_0 = (k'_{-1}\tilde{\boldsymbol{c}}_{-1} + k'_{+1}\tilde{\boldsymbol{c}}_{+1} + k'_2\tilde{\boldsymbol{c}}_2) - (k_{+1}\tilde{\boldsymbol{c}}_0 + k_{-1}\tilde{\boldsymbol{c}}_0 + k_2\tilde{\boldsymbol{c}}_0) + D_0\frac{1}{r}\frac{\partial}{\partial r}\left[r\frac{\partial\tilde{\boldsymbol{c}}_0}{\partial r}\right] \quad (1a)$$

$$\partial_t\tilde{\boldsymbol{c}}_{+1} = (k_{+1}\tilde{\boldsymbol{c}}_0 - k'_{+1}\tilde{\boldsymbol{c}}_{+1}) - \frac{V_{+1}}{r}\frac{\partial(\tilde{\boldsymbol{c}}_{+1}r)}{\partial r} \quad (1b)$$

$$\partial_t\tilde{\boldsymbol{c}}_{-1} = (k_{-1}\tilde{\boldsymbol{c}}_0 - k'_{-1}\tilde{\boldsymbol{c}}_{-1}) - \frac{V_{-1}}{r}\frac{\partial(\tilde{\boldsymbol{c}}_{-1}r)}{\partial r} \quad (1c)$$

$$\partial_t\tilde{\boldsymbol{c}}_2 = (k_2\tilde{\boldsymbol{c}}_0 - k'_2\tilde{\boldsymbol{c}}_2) + D_2\frac{1}{r}\frac{\partial}{\partial r}\left[r\frac{\partial\tilde{\boldsymbol{c}}_2}{\partial r}\right]. \quad (1d)$$

In most cells, the velocities of microtubule-dependent transport of organelles are roughly equal in both directions, $V_{+1} \approx -V_{-1} \approx V$ (1,3,10). The above system of equations can be approximated with an advection-diffusion equation for the total density of organelles, $\tilde{c}(r,t) = \sum\tilde{c}_s(r,t)$(9). After nondimensionalization, this equation yields

$$\Pi\frac{\partial c}{d\tau} \approx \Phi\frac{1}{\xi}\frac{\partial(c\xi)}{\partial\xi} + \Omega\frac{1}{\xi}\frac{\partial^2(c\xi)}{\partial\xi^2} + \Delta\frac{1}{\xi}\frac{\partial}{\partial\xi}\left[\xi\frac{\partial c}{\partial\xi}\right], \quad (2)$$

where

$\xi = r/R_C$, $\xi_N = R_N/R_C$, $\tau = tV/R_C$, $c = \tilde{c}/C_0$,
$\Pi = 1 + K_{+1} + K_{-1} + K_2$, $\Phi = K_{-1} - K_{+1}$, $\Delta = \tilde{D}_2K_2 + \tilde{D}_0$,

$$\Omega = \frac{V}{R_C}\left(\frac{K_{+1}}{k'_{+1}}\left(1+\frac{\Phi}{\Pi}\right)^2 + \frac{K_{-1}}{k'_{-1}}\left(1-\frac{\Phi}{\Pi}\right)^2 + \frac{K_2}{k'_2}\left(\frac{\Phi}{\Pi}\right)^2\right),$$

$\tilde{D}_2 = D_2/VR_C$ and $\tilde{D}_0 = D_0/VR_C$.

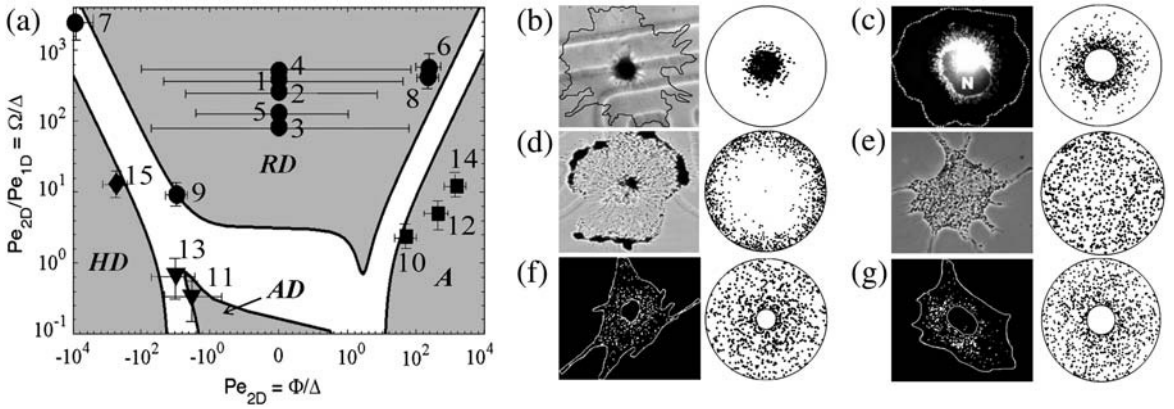

FIGURE 2 (*a*) Regime map of organelle patterns. Data points labeled [1–3] represent endosomes containing dextran [1], low density lipoprotein [2], polyethylenimine-DNA [3] in human fibroblasts (1); [4] free (nonperinuclear) lysosomes in human fibroblasts; [5] peroxisomes in COS-7 and HepG2 (9); [6] secretory vesicles in PC12 cells (10); [7–8] exocytotic vesicles in control [7] and tau-transfected [8] CHO cells (11); [9–10] mitochondria in control [9] and tau-transfected [10] CHO cells (11), [11–12] melanosomes in frog melanophores when stimulated for areal dispersion [11] and aggregation [12] (2,8,12); [13–14] melanosomes in fish melanophores when stimulated for areal dispersion [13] and aggregation [14] (2,8,12); [15] melanosomes in fish melanophores treated with an AF-disrupting drug and stimulated for areal dispersion [3]. The large error bars on points [1–5] are due to the logarithmic nature of the regime map. Shaded regions correspond to limiting stationary patterns (*A*, aggregation; *AD*, areal dispersion; *HD*, hyperdispersion; and *RD*, radial dispersion). Open regions represent transitions among these patterns and cannot be assigned to any particular pattern. (*b–g*) Comparison between predicted (*right*) and experimentally observed organelle patterns (*left*) for (*b*) melanosomes in fish melanophores when stimulated with melatonin (3), (*c*) mitochondria in tau-transfected CHO cells (11), (*d*) melanosomes in fish melanophores after treated with an AF-disrupting drug and stimulated for areal dispersion (3), (*e*) melansomes in Xenopus melanophores when stimulated for areal dispersion (3), (*f*) endosomes in human fibroblasts (1), and (*g*) peroxisomes in Drosophila S2 (13). See Supplementary Material for more information.

Equation 2 demonstrates contributions of three principal types of organelle motions: i), biased directed motions on MTs, represented by Φ, either toward ($\Phi > 0$) or away ($\Phi < 0$) from the nucleus; ii), dispersive motions of organelles along the radial coordinate originating from their random walks in both directions on MTs (1), represented by Ω; and iii), dispersive motions of organelles over the cell surface due to combined actions of diffusion in cytosol and myosin-dependent movements on AFs, represented by Δ. The equilibrium spatial distribution of organelles is determined by the relative contributions of each type of motion. To quantify this, we define two dimensionless groups. The first group, one-dimensional Peclet number $Pe_{1D} = \Phi/\Omega$, compares the timescales of convective and diffusive motion on MTs. The second group, two-dimensional Peclet number $Pe_{2D} = \Phi/\Delta$, compares the time scales of convective motion on MTs and diffusive motion over cell surface. Parameters necessary to calculate both Peclet numbers are obtained from independent experiments in literature (see Supplementary Material).

Equation 2 was numerically solved for a wide range of Peclet number values to determine the patterns at steady-state. We identify four distinct limiting patterns: i), aggregation, accumulation of organelles near the cell center (Fig. 2, *b* and *c*); ii), hyperdispersion, concentration of organelles near the cell periphery (Fig. 2 *d*); iii); areal dispersion, uniform distribution of organelles over the cell surface area (Fig. 2 *e*); and iv), radial dispersion, uniform distribution of organelles along the radial coordinate (Fig. 2, *f* and *g*). We then construct a regime map for the patterns based on quantitative characterization of the organelle distributions (e.g., mean distance to the cell center, or deviations from the uniform distribution; see Supplementary Material). The regime map, depicted in Fig.2 *a*, establishes a simple relationship between motor activities (the cause), represented here by the two Peclet numbers, and intracellular distributions of organelles (the effect). It provides a quantitative and direct method for classifying patterns of many important organelles inside cells. The patterns predicted by the model were found to be in good agreement with those occurring in nature, showing that organelle organization in cells is indeed an emergent property of interactions of components at microscopic/molecular level.

In summary, we report a generalized theoretical model for ''flows'' of organelles inside cells and identify two dimensionless numbers that control the regimes of the flow patterns. Using three fundamental motions, mediated by kinesin, dynein, and myosin, cells elegantly generate a variety of organelle organization at a microscopic level, adapted to the needs of the organisms. Interestingly, the regime map reveals that radial dispersion is the desired distribution of many intracellular organelles under normal operating conditions. Such a simple organization principle, based on a delicate balance between kinesin and dynein activities, allows the cell to maintain a robust and well-defined spatial organization of organelles against perturbations in operating environments. Interactions between organelles, such as fusion and mutual exclusion, are not considered in the theory presented here and can give rise to interesting, nonlinear behaviors (5). Further work can provide important clues about the underlying principles of organelle organization and a better understanding of diseases related to organelle transport. In this sense, the theory provides a stepping stone toward a realistic, systematic, and quantitative description of intracellular transport.

SUPPLEMENTARY MATERIAL

An online supplement to this article can be found by visiting BJ Online at http://www.biophysj.org.

REFERENCES and FOOTNOTES

1. Pangarkar, C., A. T. Dinh, and S. Mitragotri. 2005. Dynamics and spatial organization of endosomes in mammalian cells. *Phys. Rev. Lett.* 95:158101.
2. Nascimento, A. A., J. T. Roland, and V. I. Gelfand. 2003. Pigment cells: a model for the study of organelle transport. *Annu. Rev. Cell Dev. Biol.* 19:469–491.
3. Rodionov, V., J. Yi, A. Kashina, A. Oladipo, and S. P. Gross. 2003. Switching between microtubule- and actin-based transport systems in melanophores is controlled by cAMP levels. *Curr. Biol.* 13:1837–1847.
4. Snider, J., F. Lin, N. Zahedi, V. Rodionov, C. C. Yu, and S. P. Gross. 2004. Intracellular actin-based transport: how far you go depends on how often you switch. *Proc. Natl. Acad. Sci. USA.* 101:13204–13209.
5. Klumpp, S., T. M. Nieuwenhuizen, and R. Lipowsky. 2005. Self-organized density patterns of molecular motors in arrays of cytoskeletal filaments. *Biophys. J.* 88:3118–3132.
6. Nedelec, F., T. Surrey, and A. C. Maggs. 2001. Dynamic concentration of motors in microtubule arrays. *Phys. Rev. Lett.* 86:3192–3195.
7. Dinh, A. T., T. Theofanous, and S. Mitragotri. 2005. A model for intracellular trafficking of adenoviral vectors. *Biophys. J.* 89:1574–1588.
8. Smith, D. A., and R. M. Simmons. 2001. Models of motor-assisted transport of intracellular particles. *Biophys. J.* 80:45–68.
9. Maly, I. V. 2002. A stochastic model for patterning of the cytoplasm by the saltatory movement. *J. Theor. Biol.* 216:59–71.
10. Zaliapin, I., I. Semenova, A. Kashina, and V. Rodionov. 2005. Multiscale trend analysis of microtubule transport in melanophores. *Biophys. J.* 88:4008–4016.
11. Schrader, M., M. Thiemann, and H. D. Fahimi. 2003. Peroxisomal motility and interaction with microtubules. *Microsc. Res. Tech.* 61:171–178.
12. Schutz, G. J., M. Axmann, S. Freudenthaler, H. Schindler, K. Kandror, J. C. Roder, and A. Jeromin. 2004. Visualization of vesicle transport along and between distinct pathways in neurites of living cells. *Microsc. Res. Tech.* 63:159–167.
13. Trinczek, B., A. Ebneth, E. M. Mandelkow, and E. Mandelkow. 1999. Tau regulates the attachment/detachment but not the speed of motors in microtubule-dependent transport of single vesicles and organelles. *J. Cell Sci.* 112:2355–2367.
14. Gross, S. P., M. C. Tuma, S. W. Deacon, A. S. Serpinskaya, A. R. Reilein, and V. I. Gelfand. 2002. Interactions and regulation of molecular motors in *Xenopus* melanophores. *J. Cell Biol.* 156:855–865.
15. Simpson, J. C., R. Wellenreuther, A. Poustka, R. Pepperkok, and S. Wiemann. 2000. Systematic subcellular localization of novel proteins identified by large-scale cDNA sequencing. *EMBO Rep.* 287–292.